A Minmax Approach to Adaptive Matched Field Processing in an Uncertain Propagation Environment

James C. Preisig

Abstract—**Adaptive array processing algorithms have achieved widespread use because they are very effective at rejecting unwanted signals (i.e., controlling sidelobe levels) and in general have very good resolution (i.e., have narrow mainlobes). However, many adaptive high-resolution array processing algorithms suffer a significant degradation in performance in the presence of environmental mismatch. This sensitivity to environmental mismatch is of particular concern in problems such as long-range acoustic array processing in the ocean where the array processor's knowledge of the propagation characteristics of the ocean is imperfect. An adaptive minmax matched field processor is formulated which combines adaptive matched field processing and minmax approximation techniques to achieve the effective interference rejection characteristic of adaptive processors, while limiting the sensitivity of the processor to environmental mismatch. An efficient implementation and alternative interpretation of the processor are developed. The performance of the processor is analyzed using numerical simulations.**

I. Introduction

THE signals received by spatial arrays of sensors are often composed of the sum of signals emitted by both point and spatially spread sources at different locations. In order to estimate the signal, or the parameters of the signal, emitted by a source at a particular location, the array processor must often separate that signal from the other signals which are received. The separation of signals based upon the location of the source is referred to as spatial filtering.

Array processors achieve spatial discrimination through filtering by exploiting the fact that the spatial characteristics of a propagating signal as received at an array of sensors depend upon the location of the source of the signal. However, the spatial characteristics of a propagating signal also depend upon the characteristics of the medium through which the signal is propagating. Therefore, if a processor has inaccurate or incomplete information concerning the characteristics of the propagation environment, it may be unable to determine the spatial characteristics which should be exhibited by a signal emitted by a source at the location of interest. Thus, the environmental mismatch may result in a signal model mismatch. In these cases, the processor may have difficulty in accomplishing the spatial filtering necessary to estimate the parameters of the signal of interest.

Adaptive array processors have achieved widespead use because of their good resolution and their ability to adjust their sidelobe pattern to minimize interference from noise sources. However, they have also been shown to be very sensitive to the signal model mismatch caused by environmental mismatch [1]–[3]. In ocean acoustic array processing problems where it is impractical for the processor to access detailed and precise environmental information, this sensitivity poses a serious problem. This paper proposes an approach to array processing which yields a processor capable of operating with only approximate environmental information, while at the same time achieving levels of spatial resoltuion close to those achieved by adaptive processors having accurate and detailed environmental information.

The processor, which is referred to as the adaptive minmax matched field processor, is developed within the framework of minmax signal processing. Given a range of environmental conditions over which the processor is expected to operate, the weights of the processor's linear weight-and-sum beamformer are adaptively adjusted to minimize the worst case processor error criterion evaluated over this range of environmental conditions. Thus, rather than needing precise information as to the state of the propagation environment, the processor can operate effectively when it knows only that the environmental conditions fall within a reasonable range. The details of the minmax framework, error criterion, and the proposed array processor are covered in Section III.

While the processor has its foundation in the framework of minmax signal processing, it can also be shown to be equivalent to both a particular type of Wiener filter and a combined signal model estimator and minimum variance distortionless response (MVDR) array procedssor [4], [5] (also referred to as the maximum likelihood array processor). The Wiener filter relationship is used to develop an efficient algorithm for implementing the matched field processor. The MVDR processor interpretation of the minimax processor is developed in Section IV and leads to a slight modification of the algorithm.

The signal model used throughout this paper is described in Section II. Numerical results generated using a normal

Manuscript received July 10, 1992; revised July 2, 1993. This work was supported in part by the Defense Advanced Research Projects Agency monitored by the Office of Naval Research under Grant N00014-89-J-1489 and in part by the Office of Naval Research under Grants N00014-90-452 and N00014-91-J-1628. This paper is WHOI Contribution Number 8106. The associate editor coordinating the review of this paper and approving it for publication was Prof. John A. Stuller.

The author was with the Research Laboratory of Electronics, Massachusetts Institute of Technology, Cambridge, MA. He is now with the Department of Applied Ocean Physics and Engineering, Woods Hole Oceanographic Institution, Woods Hole, MA 02543.

IEEE Log Number 9400384.

mode propagation model and a simple class of environmental uncertainty are presented and analyzed in Section V.

II. Signal Model

The signal received by the array of sensors is assumed to be the sum of uncorrelated wide-sense stationary signals emitted by point sources ($x(t,\zeta)$ where ζ is the source location), signals emitted by spatially spread sources such as breaking waves on the ocean surface, and sensor noise. The individual frequency components of each point source signal can be expressed as

$$x(t,\zeta) = A(f,\zeta)e^{j2\pi ft}$$

where the $A(f,\zeta)$ are uncorrelated, zero-mean, complex random variables with a variance of $\sigma^2(f,\zeta)$. For the purposes of this paper, the point and spatially spread sources are assumed to emit narrow-band signals.

The signal emitted by the point source at location ζ_i and received at the array of sensors will be denoted by the vector time series $\boldsymbol{x}(t,\zeta_i)$ and can expressed as

$$\boldsymbol{x}(t,\zeta_i) = A(f,\zeta_i)\boldsymbol{q}(f,\zeta_i,\boldsymbol{\phi})e^{j2\pi ft}. \tag{1}$$

Vector quantities are denoted by boldface. $\boldsymbol{q}(f,\zeta,\phi)$ is the signal replica vector which accounts for the apparent attenuation and phase delay in the sum of the signals which propagate along each of the possibly multiple paths from the source to each array sensor. Here, it is assumed that the environment is time-invariant. This assumption is reasonable when the time scale of environmental change is much longer than the observation interval. $\boldsymbol{\phi}$ is a vector of parameters used to describe relevant characteristics of the propagation enviornment. Thus, the spatial structure exploited by the array processor to achieve spatial discrimination is quantified by the signal replica vector.

The received signal, denoted by the vector time series $\boldsymbol{y}(t)$, is then given by

$$\begin{aligned}\boldsymbol{y}(t) &= \sum_i \boldsymbol{x}(t,\zeta_i) + \boldsymbol{n}(t)\\ &= e^{j2\pi ft}\sum_i A(f,\zeta_i)\boldsymbol{q}(f,\zeta_i,\boldsymbol{\phi}) + \boldsymbol{n}(t)\end{aligned} \tag{2}$$

where $\boldsymbol{n}(t)$ is the sum of the propagating background noise emitted by spatial spread sources, sensor noise, and signals emitted by point sources as frequencies other than f.

III. Minmax Array Processing

A. The Minmax Signal Processing Framework

The adaptive minmax matched field processor is developed within the framework of minmax signal processing. In general terms, the framework addresses the problem of developing a processor whose worst case performance evaluated over a given class and range of uncertainties is as favorable as possible. Specifically, let $g(\boldsymbol{y},\boldsymbol{w})$ be a processor parameterized by the vector $\boldsymbol{w}$ which maps an observed signal ($\boldsymbol{y}$) to an estimate of some signal or parameter of interest ($\boldsymbol{x}$ where $\hat{\boldsymbol{x}}$ denotes an estimate of the vector $\boldsymbol{x}$). The set of allowable values for the parameter vector $\boldsymbol{w}$ is denoted by W. For example, if $g(\boldsymbol{y},\boldsymbol{w})$ is a linear beamformer for an N-element array, the vector $\boldsymbol{w}$ contains the filter weights, and W is the space of the N -dimensional complex numbers $\mathcal{C}^N$.

The parameters which are not of direct interest but which affect the characteristics of $\boldsymbol{x}$ or $\boldsymbol{y}$, or those which govern the relationship between the observed signal and the signal or parameter of interst are referred to as the environmental parameters and will be denoted by the vector ϕ.

The ability of any particular processor as determined by the choice of $\boldsymbol{w}$ to estimate $\boldsymbol{x}$ depends upon the particular environmental condition under which the processor operates. Thus, a particular value of $\boldsymbol{w}$ which yields good processor performance under one environmental condition may yield very poor performance under another environmental condition. In the problem of interest here, a set of array weights which yield good performance if the signal emitted by a source at the location of interest has one particular signal replica vector (corresponding to a particular set of environmental conditions) may yield very poor results if that signal has another signal replica vector. A real-valued error function $\varepsilon(\boldsymbol{w},\boldsymbol{\phi})$ is used as a figure of merit to evaluate the performance of any particular processor operating under any particular environmental condition.

Under the assumption that $\varepsilon(\boldsymbol{w},\boldsymbol{\phi})$ is a continuous function of $\boldsymbol{\phi}$ for every $\boldsymbol{w} \in W$ and Φ is a compact set contained in a metric space, the extremal value for the processor parameter vector $\boldsymbol{w}$, denoted by $\Delta(\boldsymbol{w})$, is the worst case performance of the processor over the range of the environmental parameters. That is,

$$\Delta(\boldsymbol{w}) \triangleq \max_{\boldsymbol{\phi}\in\Phi} \varepsilon(\boldsymbol{w},\boldsymbol{\phi}).$$

The optimal minmax processor parameter vector is then defined as that which minimizes this extremal value. That is,

$$\boldsymbol{w}_{\text{opt}} \triangleq \arg\min_{\boldsymbol{w}\in W} = \Delta(\boldsymbol{w}) = \arg\min_{\boldsymbol{w}\in W}\max_{\boldsymbol{\phi}\in\Phi} \varepsilon,(\boldsymbol{w},\boldsymbol{\phi}).$$

The extremal point set, denoted by $M(\boldsymbol{w})$, is the set of all extremal points. That is,

$$M(\boldsymbol{w}) \triangleq \{\boldsymbol{\phi} \in \Phi | \varepsilon(\boldsymbol{w},\boldsymbol{\phi}) = \Delta(\boldsymbol{w})\}.$$

The use of minmax signal processing techniques to deal with uncertainty in environmental parameters has been proposed previously. Examples of such techniques and much of the theoretical development of minmax techniques are contained in [6]–[10]. Recently published work [11] applied this theory in the context of matched field processing by developing a minmax matched filtering technique. Unlike the processor developed herein, that technique uses a nonadaptive filtering approach, and thus does not realize the potential for improved interference rejection offered by adaptive techniques.

B. The Adaptive Minmax Matched Field Processor

1) Processor Structure: The adaptive minmax matched field processor takes as its input the time-sampled signal

received by an array of sensors which has been low-pass filtered prior to sampling to prevent frequency domain aliasing. This input is denoted by the discrete-time vector time series $\boldsymbol{y}[m]$. Consistent with the notation in Section II, the vector time series $\boldsymbol{x}[m,\zeta]$ denotes the time-sampled received signal which was emitted by a point source at a position ζ.$\boldsymbol{n}[m]$ denotes the interfering noise from various sources.

Equation (1) can be manipulated to yield

$$\boldsymbol{x}[m,\zeta] = x_d[m,f,\zeta]\tilde{\boldsymbol{q}}(f,\zeta,\boldsymbol{\phi})$$

where

$$\tilde{\boldsymbol{q}}(f,\zeta,\boldsymbol{\phi}) = \frac{q_k^*(f,\zeta,\boldsymbol{\phi})}{|q_k(f,\zeta,\boldsymbol{\phi})|}\frac{\boldsymbol{q}(f,\zeta,\boldsymbol{\phi})}{|\boldsymbol{q}(f,\zeta,\boldsymbol{\phi})|} \tag{3}$$

and

$$x_d[m,f,\zeta] = e^{j2\pi f m\tau_s}A(f,\zeta)|\boldsymbol{q}(f,\zeta,\boldsymbol{\phi})|\frac{q_k(f,\zeta,\boldsymbol{\phi})}{|q_k(f,\zeta,\boldsymbol{\phi})|}. \tag{4}$$

Here, the superscript * denotes complex conjugate, τ_s is the sampling period, $\tilde{\boldsymbol{q}}(f,\zeta,\boldsymbol{\phi})$ is the normalized signal replica vector, and $x_d[m,f,\zeta]$ is the desired signal. The first factor in (3) normalizes the phase so that the arbitrarily selected kth term of the normalized replica vector is real and nonnegative. The denominator of the second term normalizes the magnitude of the replica vector to equal one. The phase normalization allows the processor to estimate $x_d[m,f,\zeta]$ by exploiting the phase differences between the signal as received at each sensor in the array without having to account for common fluctuations in the signal travel time between the source and each sensor.

The quantity estimated by the processor is the average power in the desired signal at a selected frequency emitted by a source at a location of interest. The average power is given by

$$\sigma_d^2(f,\zeta) = |A(f,\zeta)|^2|\boldsymbol{q}(f,\zeta,\boldsymbol{\phi})|^2.$$

The location of interest is referred to as the array focal point. Here, ζ is the array focal point. The desired signal is the selected frequency component of the signal emitted by a point source at the array focal point scaled to account for propagation-induced attenuation and phase shifts as given in (4). The array focal point can be swept through space, and the selected frequency can be swept through the frequency spectrum to generate an estimate $\hat{\sigma}_d^2(f,\zeta)$ of the average power in the desired signal as a function of spatial location and temporal frequency.

Conceptually, the processor which generates this estimate consists of three modules (Fig. 1). The first module divides the time-sampled signal received by the array $\boldsymbol{y}[m]$ into segments M samples in length, and computes the vector discrete-time Fourier transform of each segment at the selected frequency given by

$$\boldsymbol{Y}^l(f) = \frac{1}{M}\sum_{m=0}^{M-1}\boldsymbol{y}^l[m]e^{-j2\pi f m\tau_s} \tag{5}$$

where l indicates the segment number, $\boldsymbol{y}^l[m]$ is the mth sample of the lth segment, and the term $1/M$ is a normalization

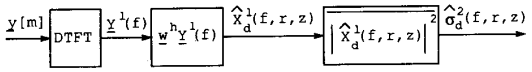

Fig. 1. Adaptive minmax MFP structure.

term. Here, f is the frequency expressed in cycles per second which satisfies $|f| \le 1/2\tau_s$.

Ignoring the spectral leakage from adjacent frequency components due to the finite length of the segments, (2) and (5) can be combined to yield

$$\begin{aligned}\boldsymbol{Y}^l(f) &= \sum_{\zeta}\boldsymbol{X}^l(f,\zeta) + \boldsymbol{N}^l(f)\\ &= \sum_{\zeta}X_d^l(f,\zeta)\tilde{\boldsymbol{q}}(f,\zeta,\boldsymbol{\phi}) + \boldsymbol{N}^l(f)\end{aligned}$$

where

$$X_d^l(f,\zeta) = A(f,\zeta)|\boldsymbol{q}(f,\zeta,\boldsymbol{\phi})|\frac{q_k(f,\zeta,\boldsymbol{\phi})}{|q_k(f,\zeta,\boldsymbol{\phi})|}. \tag{6}$$

The summation is over the locations of the point sources. The transformed segments are known as "snapshots" and $\boldsymbol{X}^l(f,\zeta)$ denotes the snapshot of the lth segment of $\boldsymbol{x}[m,\zeta]$.$Y_i^l(f)$ denotes the snapshot of the lth segment of the signal received by the ith array sensor and $X_d^l(f,\zeta)$ denotes the snapshot of the desired signal. The phase term in $X_d^l(f,\zeta)$ which results from the shifting of the time origin for the Fourier transform of each segment has been dropped in (6) because it has no effect on the performance of the array processor.

The snapshots of the received signal are the inputs to the second module which is a linear weight-and-sum beamformer. This beamformer computes an estimate of the snapshot of the lth segment of the desired signal using

$$\hat{X}_d^l(f,\zeta) = \boldsymbol{w}^h\boldsymbol{Y}^l(f) \tag{7}$$

where w is the array weight vector and the superscript h denotes Hermitian. The final module computes an estimate of the average power in the desired signal. The overbar in Fig. 1 indicates the sample mean taken over all l. That is, if L is the number of segments used in estimating $\sigma_d^2(f,\zeta)$, then

$$\hat{\sigma}_d^2(f,\zeta) = \frac{1}{L}\sum_{l=1}^{L}|\hat{X}_d^l(f,\zeta)|^2. \tag{8}$$

While this structure is the same as that used by many array processors, such as Capon's MVDR processor, the unique feature of this processor is the manner in which the array weight vector $\boldsymbol{w}$ is calculated. For this processor, the array weight vector is the solution to a minmax optimization problem where the error ε is a meausre of the spatial filter's ability to pass the desired signal without distortion while rejecting the interfering signals in a given propagation environment.

2) The Minmax Array Weights: For any particular array focal point, frequency, array weight vector, and propagation environment, the error function for the adaptive minmax matched field processor is the *a priori* mean-squared error in the estimation of $X_d(f,\zeta)$ conditioned on the characteristics

of the propagation environment, that is

$$\begin{aligned}\varepsilon(f,\zeta,\boldsymbol{w},\boldsymbol{\phi}) &= E[|X_d(f,\zeta)-\hat{X}_d(f,\zeta)|^2|\boldsymbol{\phi}] \\ &= E[|X_d(f,\zeta)-\boldsymbol{w}^h\boldsymbol{Y}(f)|^2|\boldsymbol{\phi}] \end{aligned} \quad (9)$$

where the characteristics of the propagation environment are parameterized by the vector $\boldsymbol{\phi}$.

For a given array focal point and frequency, the optimal array weights are defined as

$$\boldsymbol{w}_{\text{opt}}(f,\zeta) = \arg \min_{\boldsymbol{w}\in C^N} \max_{\boldsymbol{\phi}\in\Phi} \varepsilon(f,\zeta,\boldsymbol{w},\boldsymbol{\phi}) \quad (10)$$

where N is the number of array sensors and Φ is the user-specified range of the environmental parameters over which the processor must operate.

Under the assumption stated earlier that the desired signal and the interfering signals are uncorrelated, (9) can be rewritten as

$$\begin{aligned}\varepsilon(f,\zeta,\boldsymbol{w},\boldsymbol{\phi}) = E[X_d(f,\zeta)X_d^*(f,\zeta)X_d^*(f,\zeta)|\boldsymbol{\phi}] \\ - 2\text{Real}(E[\boldsymbol{X}(f,\zeta)X_d^*(f,\zeta)|\boldsymbol{\phi}]^h\boldsymbol{w}) \\ + \boldsymbol{w}^h E[\boldsymbol{Y}(f)\boldsymbol{Y}(f)^h|\boldsymbol{\phi}]\boldsymbol{w}. \end{aligned} \quad (11)$$

The expectation in the last term of (11) is the cross-spectral correlation matrix of the received signal conditioned on the environmental parameter $\boldsymbol{\phi}$. The cross-spectral correlation matrix is the parameterization used by the processor to characterize the spatial structure of the total signal field, and it is the input which enables the processor to adapt to reject unwanted signals. Here, the matrix will not be treated as a function of the particular environmental conditions or the characteristics of any particular propagating signal. Instead, it will be treated as a property of the total signal field. Therefore, the conditioning of the expectation in the last term of (11) is dropped and the actual ensemble cross-spectral correlation matrix $S(f)$ is used. In most cases, this ensemble cross-spectral correlation matrix is unknown to the processor. Therefore, the sample cross-spectral correlation matrix given by $\hat{S}(f) \triangleq (1/L)\Sigma_{l=1}^{L}\boldsymbol{Y}^l(f)\boldsymbol{Y}^l(f)^h$ will be substituted for $S(f)$. Nothing in the derivation of the algorithm in the remainder paper depends upon this substitution.

Assuming that the environmental processes which cause changes in the signal replica vector and the signal source phase and amplitude term $A(f,\zeta)$ are statistically independent, the expectation in the second term of (11) can be expressed as

$$E[X_d(f,\zeta)X_d^*(f,\zeta)|\boldsymbol{\phi}]E[\tilde{\boldsymbol{q}}(f,\zeta,\phi)|\boldsymbol{\phi}]. \quad (12)$$

Herein, the normalized signal replica vector will be assumed to be uniquely determined by the environmental parameters $\boldsymbol{\phi}$. Given this assumption, the expectation in the second factor of (12) can be removed.

In realistic ocean environments, the normalized signal replica vector is not uniquely determined by a finite set of parameters. It is possible to calculate the conditional expectation of the normalized signal replica vector as a function of the temporal and spatial condition cross-correlation function of the propagating signal where the conditioning is on the parameter vector $\boldsymbol{\phi}$ [12]. Extensive literature has been published relating the characteristics of ocean processes to the cross-correlation functions required to compute the conditional expectation of the normalized signal replica vector. Examples of two different approaches are contained in [13]–[15]. While the above assumption of a unique relationship between the normalized signal vector and the environmental parameter vector $\boldsymbol{\phi}$ is not valid in realistic ocean environments, the essential results of this work are not affected by this assumption.

The expression $E[X_d(f,\zeta)X_d^*(f,\zeta)|\boldsymbol{\phi}]$ appears in the first term of (11) and in (12). This expression is the conditional average power in the desired signal, and will be replaced by the actual average power in the desired signal $\sigma_d^2(f,\zeta) \triangleq E[X_d(f,\zeta)X_d^*(f,\zeta)]$. Given the factorization and the substitutions detailed above, the error criterion can be expressed as

$$\varepsilon(f,\zeta,\boldsymbol{w},\boldsymbol{\phi},\sigma_d^2) = \sigma_d^2 - 2\sigma_d^2\,\text{Real}(\tilde{\boldsymbol{q}}^h(f,\zeta,\boldsymbol{\phi})\boldsymbol{w}) + \boldsymbol{w}^h\hat{S}(f)\boldsymbol{w} \quad (13)$$

where the dependence of the error on the average power in the desired signal is explicitly shown and the dependence of the average power on the frequency and focal point has been suppressed for notational convenience.

The optimal array weights minimize the maximum value of this error evaulated over the operating range of the environmental parameters. Conceptually, they can be considered those of a data-adaptive Wiener filter which is robust with respect to changes in the spatial correlation of the signal to be estimated.

3) Characterization of $\boldsymbol{w}_{\text{opt}}(f,\zeta,\sigma_d^2)$*:* From (10), the minmax problem which must be solved is

$$\boldsymbol{w}_{\text{opt}}(f,\zeta,\sigma_d^2) = \arg \min_{\boldsymbol{w}\in C^N} \max_{\boldsymbol{\phi}\in\Phi} \varepsilon(f,\zeta,\boldsymbol{w},\boldsymbol{\phi},\sigma_d^2)$$

where $\varepsilon(f,\zeta,\boldsymbol{w},\phi,\sigma_d^2)$ is given in (13).

The following characterization theorem for the minmax array weight problem states the necessary and sufficient conditions satisfied by $w_{\text{opt}}(f,\zeta,\sigma_d^2)$. A proof of this theorem is contained in [12]. In (16), the notation $\mathcal{H}(\{\})$ denotes the convex hull[1] of the vectors contained in the set $\{\}$ and $\boldsymbol{0}$ is the vector of zeros.

Array Weight Characterization Theorem: Let Φ be a compact set contained in a metric space, and let $\tilde{\boldsymbol{q}}(f,\zeta,\boldsymbol{\phi})$ be a continuous function on Φ. Then, a necessary and sufficient condition for w_0 to be a solution to the minmax problem

$$\boldsymbol{w}_{\text{opt}}(f,\zeta,\sigma_d^2) = \arg \min_{\boldsymbol{w}\in C^N} \max_{\boldsymbol{\phi}\in\Phi} \varepsilon(f,\zeta,\boldsymbol{w},\boldsymbol{\phi},\sigma_d^2)$$

is that

$$\exists J > 0 \quad (14)$$

and

$$\exists \tilde{M}(\boldsymbol{w}_0) = \{\boldsymbol{\phi}_1,\cdots,\boldsymbol{\phi}_J\} \subseteq M(\boldsymbol{w}_0) \quad (15)$$

such that

$$\boldsymbol{0} \in \mathcal{H}(\{(\hat{S}(f)\boldsymbol{w}_0 - \sigma_d^2\tilde{\boldsymbol{q}}(f,\zeta,\boldsymbol{\phi}))|\boldsymbol{\phi}\in\tilde{M}(\boldsymbol{w}_0)\}). \quad (16)$$

[1]The convex hull of a set of vectors is the larger set of vectors which are expressible as a convex combination of the vectors in the original set. That is, if $A = \{\boldsymbol{\alpha}_1,\cdots,\boldsymbol{\alpha}_J\}$, then $\mathcal{H}(A) = \{\boldsymbol{\alpha}|\exists p_1,\cdots,p_J; \Sigma_{i=1}^{J}p_i = 1; p_i \geq 0;$ and $\boldsymbol{\alpha} = \Sigma_{i=1}^{J}p_i\boldsymbol{\alpha}_i\}$.

An upper bound can be placed on the number of extermal points which must be simultaneously considered in testing for or constructing an optimal solution. In [12], it is shown that $\boldsymbol{w}_0$ is a solution as described above if and only if $\exists J \in \{1, \cdots, 2N+1\}$ for which (15) and (16) are satisfied. Thus, while it may be possible to find multiple sets of extremal points satisfying (15) and (16), at least one of these sets will contain only $2N+1$ or fewer elements.

Equation (16) is satisified if and only if $\exists p_1, \cdots, p_J$ such that $p_i \geq 0, \Sigma_{i-1}^{J} p_i = 1$, and

$$\mathbf{0} = \sum_{i=1}^{J} p_i (\hat{S}(f)\boldsymbol{w}_o - \sigma_d^2 \tilde{\boldsymbol{q}}(f, \zeta, \boldsymbol{\phi}_i)). \tag{17}$$

Manipulation of (17) yields the following expression for $\boldsymbol{w}_{\text{opt}}(f, \zeta, \sigma_d^2)$:

$$\boldsymbol{w}_{\text{opt}}(f, \zeta, \sigma_d^2) = \sigma_d^2 \hat{S}(f)^{-1} \sum_{i=1}^{J} p_i \tilde{\boldsymbol{q}}(f, \zeta, \boldsymbol{\phi}_i). \tag{18}$$

Therefore, if the appropriate set of extremal points and convex weights can be determined, the optimal array weight vector can be calculated directly. The minmax problem can therefore be reformulated as jointly finding the $\boldsymbol{w}_{\text{opt}}(f, \zeta, \sigma_d^2) \in \mathcal{C}^N, J, \boldsymbol{\phi}_1, \cdots, \boldsymbol{\phi}_J$, and $p_1, \cdots, p_J$ which satisfy (18). The key to finding the appropriate set of extremal points, convex weights, and array weight vector lies in reformulating the minmax estimation problem as a Wiener filtering problem with the uncertain environmental parameter treated as a random parameter.

4) The Least Favorable pmf Random Parameter Framework: For most classes of realistic environmental uncertainty, the error function $\varepsilon : \mathcal{C}^N x \Phi \rightarrow \mathbb{R}$ does not contain a saddlepoint solution (see [10] for a definition and discussion of saddlepoint solutions). However, following what is referred to as a randomizing startegy in [10], the original minmax problem can be recast as a minmax problem for which a saddlepoint does exist.

The randomizing startegy is to interpret the uncertain environmental parameter as a random parameter with a particular probability distribution. The conditional mean-squared error $\varepsilon(f, \psi, \boldsymbol{w}, \boldsymbol{\phi}, \sigma_d^2)$ is then averaged over the environmental conditions to yield a mean-squared error. This mean-squared error does contain a saddlepoint with respect to the probability distribution and the array weights. Thus, the minimum mean-squared error (Wiener filter) array weights corresponding to the probability distribution at the saddlepoint are also the weights which minimize the maximum value of the mean-squared error evaluated over all possible probability distributions. The Least Favorable pmf theorem given in this section establishes the equivalence between this saddlepoint solution and the minmax solution to the original array weight problem.

As a computational necessity and to ensure that $\tilde{\boldsymbol{q}}(f, \zeta, \boldsymbol{\phi})$ is a continuous function on Φ, the range of the environmental parameter will be sampled (i.e., $\Phi = \{\boldsymbol{\phi}_1, \cdots, \boldsymbol{\phi}_K\}$), and the minmax problem will be solved on this discrete set of environmental conditions. Therefore, the probability function assigned to the environmental parameters will take the form of a pmf (probability mass function).

The pmf will be denoted by $\boldsymbol{p} \in \mathbb{R}^K$ and must satisfy

$$p_i \geq 0 \text{ and } \sum_{i=1}^{K} p_i = 1.$$

For any pmf and array weight vector, the mean-squared estimation error is

$$\begin{aligned} \varepsilon(f, \zeta, \boldsymbol{w}, \boldsymbol{p}, \sigma_d^2) &\triangleq E[|X_k^l(f, \zeta) - \hat{X}_k^l(f, \zeta)|^2] \\ &= \sum_{i=1}^{K} p_i \varepsilon(f, \zeta, \boldsymbol{w}, \boldsymbol{\phi}_i, \sigma_d^2). \end{aligned} \tag{19}$$

Define the minimum mean-squared error weight vector to be

$$\boldsymbol{w}_{\text{mmse}}(f, \zeta, \sigma_d^2, \boldsymbol{p}) \triangleq \arg \min_{\boldsymbol{w} \in \mathcal{C}^N} \varepsilon(f, \zeta, \boldsymbol{w}, \boldsymbol{p}, \sigma_d^2).$$

Then, substituting (13) into (19) and carrying out some algebraic manipulation yields an unconstrained and convex quadratic minimization problem for $\boldsymbol{w}_{\text{mmse}}(f, \zeta, \sigma_d^2, \boldsymbol{p})$. Defining the matrix $Q(f, \zeta)$ as $Q(f, \zeta) \triangleq [\tilde{\boldsymbol{q}}(f, \zeta, \boldsymbol{\phi}_1), \cdots, \tilde{\boldsymbol{q}}(f, \zeta, \boldsymbol{\phi}_K)]$, the solution is given by

$$\begin{aligned} \boldsymbol{w}_{\text{mmse}}(f, \zeta, \sigma_d^2, \boldsymbol{p}) &= \sigma_d^2 \hat{S}(f)^{-1} \sum_{i=1}^{K} p_i \tilde{\boldsymbol{q}}(f, \zeta, \boldsymbol{\phi}_i) \\ &= \sigma_d^2 \hat{S}(f)^{-1} Q(f, \zeta) \boldsymbol{p}. \end{aligned} \tag{20}$$

Equations (18) and (20) differ only in the respect that in (18), the summation is over J extremal points contained in $M(\boldsymbol{w}_0)$, while in (20), the summation is over all environmental conditions contained in Φ. Therefore, if a pmf p can be found such that p_i is greater than zero only if $\boldsymbol{\phi}_i \in M(\boldsymbol{w}_{\text{mmse}}(f, \zeta, \sigma_d^2, \boldsymbol{p}))$, then the summation in (20) will be over only the extremal points contained in $M(\boldsymbol{w}_{\text{mmse}}(f, \zeta, \sigma_d^2, \boldsymbol{p}))$. In this case, the sufficient conditions in the array weight characterization theorem will be satisfied by $K, p_1, \cdots, p_K, \boldsymbol{\phi}_1, \cdots, \boldsymbol{\phi}_K$, and $\boldsymbol{w}_{\text{mmse}}(f, \zeta, \sigma_d^2, \boldsymbol{p})$.

The characterization of the desired pmf is given in the following theorem. A proof of this theorem and an intuitive explanation of this result are contained in [12].

Least Favorable pmf Theorem: Let P be the set of all possible pmf's which may be assigned to Φ, and define the least favorable pmf as

$$\begin{aligned} \boldsymbol{p}_{lf} &\triangleq \arg \max_{\boldsymbol{p} \in P} \min_{\boldsymbol{w} \in \mathcal{C}^N} \varepsilon(f, \zeta, \boldsymbol{w}, \boldsymbol{p}, \sigma_d^2) \\ &= \arg \max_{\boldsymbol{p} \in P} \varepsilon(f, \zeta, \boldsymbol{w}_{\text{mmse}}(f, \zeta, \sigma_d^2, \boldsymbol{p}), \boldsymbol{p}, \sigma_d^2). \end{aligned} \tag{21}$$

Then

$$\boldsymbol{w}_{\text{opt}}(f, \zeta, \sigma_d^2) = \boldsymbol{w}_{\text{mmse}}(f, \zeta, \sigma_d^2, \boldsymbol{p}_{lf}).$$

5) Solving for the Least Favorable pmf: By combining (13), (19), and (20) and carrying out algebraic manipulation, the minimum mean-squared estimation error can be expressed as

$$\begin{aligned} &\varepsilon(f, \zeta, \boldsymbol{w}_{\text{mmse}}(f, \zeta, \sigma_d^2, \boldsymbol{p}), \boldsymbol{p}, \sigma_d^2) \\ &\quad = \sigma_d^2 (1 - \sigma_d^2 \boldsymbol{p}^t Q(f, \zeta)^h \hat{S}(f)^{-1} Q(f, \zeta) \boldsymbol{p}). \end{aligned} \tag{22}$$

Finding the $\boldsymbol{p}$ to maximize this quantity is equivalent to finding the $\boldsymbol{p}$ to minimize the matrix quadratic product in the second term. Therefore, (21) can be rewritten as

$$\begin{aligned}\boldsymbol{p}_{lf} &\triangleq \arg\max_{\boldsymbol{p}\in P}\min_{\boldsymbol{w}\in\mathcal{C}^N}\varepsilon(f,\zeta,\boldsymbol{w},\boldsymbol{p},\sigma_d^2)\\ &= \arg\min_{\substack{\boldsymbol{p}\geq 0\\ \boldsymbol{e}^t\boldsymbol{p}=1}}\boldsymbol{p}^t T(f,\zeta)\boldsymbol{p}\end{aligned}\tag{23}$$

where $T(f,\zeta)=\text{Real}(Q(f,\zeta)^h\hat{S}(f)^{-1}Q(f,\zeta))$, $\boldsymbol{e}=[1,\cdots,1]^t$, and the set P is explicitly defined.

A solution to (23) is guaranteed to exist because $\boldsymbol{p}^tT(f,\zeta)\boldsymbol{p}$ is a continuous function of p and the set P is a compact set. $T(f,\zeta)$ is a positive semi-definite symmetric matrix so $\boldsymbol{p}^tT(f,\zeta)\boldsymbol{p}$ is a convex function of p. There are a number of algorithms available for solving linearly constrained convex quadratic minimization problems such as (23).

An algorithm, based on the complementary pivot theory, was proposed by Lemke in [16] and is described in a more readable form in chapter 11 of [17]. The basic intuition behind the use of the complementary pivot theory to solve a quadratic problem is that the necessary and sufficient conditions, known as the Kuhn–Tucker conditions [17] for $\boldsymbol{p}_0$ to be a solution to the problem in (23), are a set of linear equations with one nonlinear constraint referred to as the complementary slackness condition. In concept, the complementary pivot algorithm is very similar to the simplex method [17] for solving linear programming problems, with an additional constraint on which variables can be pivoted into the basis at each iteration. This additional constraint ensures that the complementary slackness condition is met at each iteration.

For all nondegenerate systems of equations, the complementary pivot algorithm is guaranteed to converge to a solution in a finite number of iterations [18]. In most cases, the use of this algorithm is sufficient. However, should the degeneracy of the system be a concern, a modification of the complementary pivot algorithm can be used (see Section 7 of [18]). The problem considered here meets the necessary conditions stated in Theorem 2 on p. 618 of [18], which guarantees that the modified algorithm will converge to a solution in a finite number of iterations. A clear explanation of the modified algorithm is given on pp. 80 and 81 of [19].

6) Finding a Consistent σ_d^2: From the least favorable pmf theorem and (20), the optimal minmax array weights are given by

$$\boldsymbol{w}_{\text{opt}}(f,\zeta,\sigma_d^2)=\sigma_d^2\hat{S}(f)^{-1}Q(f,\zeta)\boldsymbol{p}_{lf}.\tag{24}$$

These weights depend upon σ_d^2, which is itself an unknown parameter to be estimated. Combining (7) and (8), the estimate of σ_d^2 is

$$\hat{\sigma}_d^2=\boldsymbol{w}_{opt}(f,\zeta,\sigma_d^2)\hat{S}(f)\boldsymbol{w}_{\text{opt}}(f,\zeta,\sigma_d^2).\tag{25}$$

Therefore, the optimal array weights depend upon the average power in the desired signal, and the estimate of this average power depends upon the array weights. This interdependence makes in necessary to calculate the optimal array weights and estimate the average power jointly.

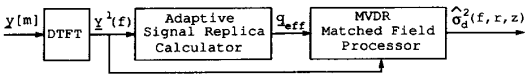

Fig. 2. Two-stage MVDR matched field processor.

This joint calculation and estimation problem is addressed by requiring that the assumed average power in the desired signal used when calculating the optimal array weights (σ_d^2 in (24) and (25)) be equal to the estimated average power in the desired signal resulting from the use of those weights ($\hat{\sigma}_d^2$ in (25)). A trivial solution to the problem is $\boldsymbol{w}_{\text{opt}}(f,\zeta,0)=\boldsymbol{0}$ and $\hat{\sigma}_d^2=0$. Since the calculation $\boldsymbol{p}_{lf}$ in (23) does not depend on σ_d^2, the nontrivial solution can be found by substituting (24) into (25) and requiring that $\sigma_d^2=\hat{\sigma}_d^2$. This yields

$$\hat{\sigma}_d^2=(\boldsymbol{p}_{lf}^tQ(f,\zeta)^h\hat{S}(f)^{-1}Q(f,\zeta)\boldsymbol{p}_{lf})^{-1}.\tag{26}$$

7) The Adaptive Minmax MFP Algorithm: The calculations in (23) and (26) and the substitution of the resulting $\hat{\sigma}_d^2$ into (24) can be combined to yield the following three-step algorithm for implementing the adaptive minmax matched field processor.

1) Use the (modified) complementary pivot algorithm to calculate

$$\boldsymbol{p}_{lf}=\arg\min_{\substack{\boldsymbol{p}\geq 0\\ \boldsymbol{e}^t\boldsymbol{p}=1}}\boldsymbol{p}^tT(f,\zeta)\boldsymbol{p}.$$

2) $\hat{\sigma}_d^2(f,\zeta)=(\boldsymbol{p}_{lf}^tT(f,\zeta)\boldsymbol{p}_{lf})^{-1}$.

3) $\boldsymbol{w}_{\text{opt}}(f,\zeta,\hat{\sigma}_d^2(f,\zeta))=\hat{\sigma}_d^2(f,\zeta)\hat{S}(f)^{-1}Q(f,\zeta)\boldsymbol{p}_{lf}$.

Here, the dependence of the average power on the frequency and array focal point is shown. Slight modifications to steps 2) and 3) of this algorithm which are motivated by the analysis in Section IV are detailed at the end of that section.

IV. The Joint Replica Estimator/MVDR Processor Interpretation of the Adaptive Minmax MFP

In Section III, the interpretation of the adaptived minmax matched field processor as a Wiener filter for the least favorable pmf led to the development of an efficient implementation of the processor. The adaptive minmax matched field processor can also be interpreted as the combination of an algorithm which calculates an effective replica vector, denoted by $\boldsymbol{q}_{\text{eff}}$, and an MVDR matched field processor which uses $\boldsymbol{q}_{\text{eff}}$ as the replica vector of the desired signal (Fig. 2). This interpretation is useful for several reasons. First, it relates the minmax array processor to an array processor whose properties are well understood. Second, it makes possible a qualitative analysis of the properties of the minmax array processor. Finally, the interpretation motivates a modification to the algorithm which improves the performance of the

As noted in Section III, the structure of the MVDR processor is identical to the structure of the adaptive minmax processor. The arrays weights of the matched field implementation of the MVDR processor [4] in a known, time-invariant environment are given by

$$\begin{aligned}\boldsymbol{w}_{\text{opt}} &= \arg\min_{\boldsymbol{w}\in\mathcal{C}^N}\boldsymbol{w}^h\hat{S}(f)\boldsymbol{w}\\ &\text{s.t.}\quad \tilde{\boldsymbol{q}}^h(f,\zeta,\boldsymbol{\phi}_0)\boldsymbol{w}=1\end{aligned}\tag{27}$$

where ϕ_0 is the parameterization of the known environmental conditions. The solution of (27) is given by

$$\boldsymbol{w}_{\text{opt}} = \frac{\hat{S}(f)^{-1}\tilde{\boldsymbol{q}}(f,\zeta,\boldsymbol{\phi}_o)}{\tilde{\boldsymbol{q}}^h(f,\zeta,\boldsymbol{\phi}_o)\hat{S}(f)^{-1}\tilde{\boldsymbol{q}}(f,\zeta,\boldsymbol{\phi}_o)}, \tag{28}$$

and the resulting estimate of the average power in the signal emitted by the source at the array focal point is

$$\hat{\sigma}_d^2(f,\zeta) = (\tilde{\boldsymbol{q}}^h(f,\zeta,\boldsymbol{\phi}_o)\hat{S}(f)^{-1}\tilde{\boldsymbol{q}}(f,\zeta,\boldsymbol{\phi}_o))^{-1}. \tag{29}$$

The relationship between the adaptive minmax matched field processor and the MVDR matched field processor is built upon the similarity between the form of the solutions in (28) and (29) and the solutions for the weights and estimated average power in steps 2) and 3) of the algorithm which implements the adaptive minmax processor.

A. The Two-Stage MVDR Matched Field Processor

The interpretation of the adaptive minmax matched field processor as the two-stage MVDR matched field processor shown in Fig. 2 is motivated by noting that the three-step algorithm detailed at the end of Section III can be rewritten as follows.

1) Use the (modified) complementary pivot algorithm to calculate

$$\boldsymbol{p}_{lf} = \arg \min_{\substack{\boldsymbol{p}\geq 0 \\ \boldsymbol{e}^t\boldsymbol{p}=1}} \boldsymbol{p}^t Q^h(f,\zeta)\hat{S}(f)^{-1}Q(f,\zeta)\boldsymbol{p}.$$

2) $\hat{\sigma}_d^2(f,\zeta) = (\boldsymbol{p}_{lf}^t Q^h(f,\zeta)\hat{S}(f)^{-1}Q(f,\zeta)\boldsymbol{p}_{lf})^{-1}$.

3) $\boldsymbol{w}_{\text{opt}}(f,\zeta,\hat{\sigma}_d^2(f,\zeta)) = \hat{\sigma}_d^2(f,\zeta)\hat{S}(f)^{-1}Q(f,\zeta)\boldsymbol{p}_{lf}$.

The set $\{Q(f,\zeta)\boldsymbol{p}|\boldsymbol{p} \geq 0 \text{ and } \boldsymbol{e}^t\boldsymbol{p} = 1\}$ is the convex hull of the set of column vectors in $Q(f,\zeta)$ (i.e., $\{\tilde{\boldsymbol{q}}(f,\zeta,\boldsymbol{\phi}_1),\cdots,\tilde{\boldsymbol{q}}(f,\zeta,\boldsymbol{\phi}_K)\}$).

Therefore, defining $\tilde{Q}(f,\zeta)$ to be the set of column vectors of $Q(f,\zeta)$, the following algorithm is equivalent to the adaptive minmax matched field processor.

1) Use the (modified) complementary pivot algorithm to calculate

$$\boldsymbol{q}_{\text{eff}} = \arg \min_{\boldsymbol{q}\in\mathcal{H}(\tilde{Q}(f,\zeta))} \boldsymbol{q}^h\hat{S}(f)^{-1}\boldsymbol{q}.$$

2) $\hat{\sigma}_d^2(f,\zeta) = (\boldsymbol{q}_{\text{eff}}^h\hat{S}(f)^{-1}\boldsymbol{q}_{\text{eff}})^{-1}$.Use the (modified) complementary pivot algorithm to calculate

$$\boldsymbol{q}_{\text{eff}} = \arg \min_{\boldsymbol{q}\in\mathcal{H}(\tilde{Q}(f,\zeta))} \boldsymbol{q}^h\hat{S}(f)^{-1}\boldsymbol{q}.$$

3) $\boldsymbol{w}_{\text{opt}}(f,\zeta,\sigma_d^2(f,\zeta)) = (\hat{S}(f)^{-1}\boldsymbol{q}_{\text{eff}}/\boldsymbol{q}_{\text{eff}}^h\hat{S}(f)^{-1}\boldsymbol{q}_{\text{eff}})$.

Steps 2) and 3) of this algorithm are the MVDR matched field processor given the replica vector $\boldsymbol{q}_{\text{eff}}$ (i.e., (28) and (29)).

From steps 1) and 2) of the two-stage MVDR matched field processor, $\boldsymbol{q}_{\text{eff}}$ is the vector contained in $\mathcal{H}(\tilde{Q}(f,\zeta))$ which maximizes the power passed through the resulting MVDR matched field processor. A detailed qualitative analysis of the adaptive minmax MFP based on this two-stage MVDR interpretation is contained in [12].

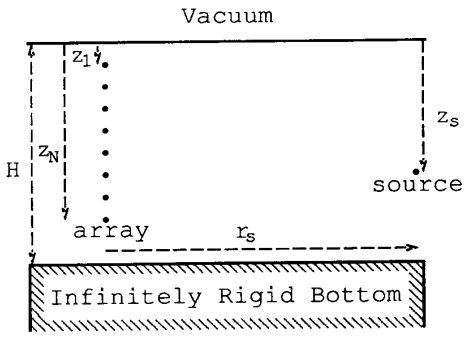

Fig. 3. Waveguide environmental model.

B. Adaptive Minmax MFP Modification

$\boldsymbol{q}_{\text{eff}}$ can be interpreted as the basis for what the processor estimates to be the rank one subspace of the signal of interest. Intuitively, the energy which the processor measures in this subspace should not depend on the norm of this basis vector. While all the vectors in $\tilde{Q}(f,\zeta)$ have a norm of one, there are vectors in $\mathcal{H}(\tilde{Q}(f,\zeta))$ with norms of less than one. This motivates a normalization of $\boldsymbol{q}_{\text{eff}}$ to have a norm of one prior to calculating the estimate of the average power or the optimal array weights. With this modification, steps 2) and 3) of the adaptive minmax MFP alogorithm become the following.

2) $\hat{\sigma}_d^2(f,\zeta) = (\boldsymbol{q}_{\text{eff}}^h\boldsymbol{q}_{\text{eff}})(\boldsymbol{q}_{\text{eff}}^h\tilde{S}(f)^{-1}\boldsymbol{q}_{\text{eff}})^{-1}$.

3) $\boldsymbol{w}_{\text{opt}}(f,\zeta,\hat{\sigma}_d^2(f,\zeta)) = (\boldsymbol{q}_{\text{eff}}^h\boldsymbol{q}_{\text{eff}})^{(1/2)}(\tilde{S}(f)^{-1}\boldsymbol{q}_{\text{eff}}/\boldsymbol{q}_{eff}^h\tilde{S}(f)^{-1}\boldsymbol{q}_{\text{eff}})$.

Numerical results generated using the modified processor are presented in the following section.

V. Numerical Performance Analysis

The performance of the adaptive minmax matched field processor is analyzed and compared to the performance of the MVDR and Bartlett matched field processors using numerical simulations. Throughout these simulations, the processors were assumed to have a perfect estimate of the cross-spectral correlation matrix $S(f)$ so Monte-Carlo type simulations are not used.

A. The Simulation Environment and Normal Mode Model

The environment used for the simulations is a range-invariant waveguide with a free surface and a rigid bottom (Fig. 3). The ocean depth (H) is 500 m. The array is a 15-element vertical array with the first sensor at 5 m depth, the 15th element at 495 m depth, and an interelement spacing of 35 m. The frequency of interest is 20 Hz. The Cartesian coordinate system of range and depth $[\zeta = (r,z)]$ is used, with the origin located at the ocean surface immediately above the array. z is positive at locations below the surface. r is the horizontal range from the array to a point and is always nonnegative. The sound speed within the waveguide is assumed to be a function of depth only and is given by the sound speed profile $c(z)$.

Let $\psi_i(z,\boldsymbol{\phi})$ be the shape of the ith normal mode of the waveguide, let $k_i(\phi)$ be the horizontal wavenumber of the

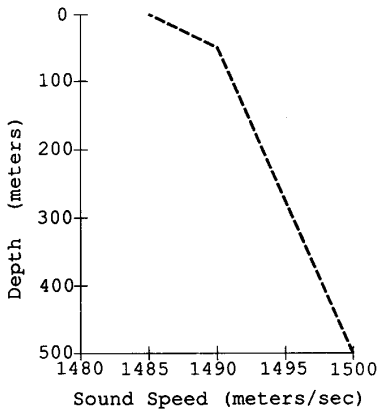

Fig. 4. Upwardly refracting sound speed profile.

ith normal mode, and assume that $|k_i(\phi)r_s|$ is large enough so that it justifies the use of a large argument approximation to the Hankel function of the second kind [20]. Then, using an adiabatic propagation model and letting $\boldsymbol{\psi}_i(\boldsymbol{\phi}) = [\psi_i(z_1, \boldsymbol{\phi}), \cdots, \psi_i(z_N, \boldsymbol{\phi})]^t$ where z_k is the depth of the kth array sensor, the signal replica vector for a source at the location (r_s, z_s) can be expressed as

$$\boldsymbol{q}(f, r_s, z_s, \boldsymbol{\phi}) = r_s^{-1/2} \sum_i \psi_i(z_s, \boldsymbol{\phi}) k_i^{-1/2}(\boldsymbol{\phi}) e^{-jk_i(\boldsymbol{\phi})r_s} \boldsymbol{\psi}_i(\boldsymbol{\phi}). \quad (30)$$

For the interested reader, a number of standard texts such as [21], [22] present a detailed treatment of adiabatic, normal-mode propagation theory.

For the values of i for which $k_i^2(\boldsymbol{\phi})$ is negative, the horizontal wavenumber will be purely imaginary with a negative coefficient and the term $e^{-jk_i(\boldsymbol{\phi})|r_s - r|}$ will decay exponentially with increasing range from the source. These modes are referred to as evanescent modes, and will be ignored due to their rapid decay. The summation in (30) can then be carried out over only the modes for which $k_i^2(\boldsymbol{\phi})$ is positive (i.e., the propagating modes).

The assumed sound speed profile is an upwardly refracting profile (Fig. 4) which is typical of the oceans at high latitudes. The sound speed profile varies linearly between a known value (1490 m/s) at a depth of 52 m and a known value (1500 m/s) at the bottom (depth of 500 m). The sound speed profile is assumed to be unknown in the top 52 m of the water column. What is known is that the sound speed profile varies linearly between an unknown value at the surface and the known value at the depth of 52 m. Therefore, the range of environmental conditions under which the processor must operate (i.e., the set Φ) is parameterized completely by the range of surface sound speeds. Throughout the tests, the adaptive minmax matched field processor was given the range of 1483–1487 m/s as the range of possible surface sound speeds. While this class of uncertainties is extremely limited, it is sufficient to demonstrate the robust performance of the mimax processor and the degradation in the performance of the MVDR and Barlett processors in the presence of environmental mismatch.

The background noise is assumed to consist of both sensor noise and propagating surface-generated noise. The sensor noise is modeled as being spatially white, and the surface-generated noise is modeled using the normal mode noise model developed in [23] and is summarized in (30) and (B7) therein. Through the simulations, the SNR with respect to the sensor noise is 20 dB and the SNR with respect to the surface generated noise is 5 dB. These SNR's are defined to be the signal-to-noise ratio in a single-frequency bin of the first-stage DTFT filter evaulated at a frequency of 20 Hz. (i.e., the SNR's are evaluated after the signal has passed through the DTFT filter.)

The results for tests of several principle attributes of the processors are presented here. These are the sensitivity to environmental mismatch and the required sampling density of the uncertainty set Φ (Section V-B), and the spatial resolution of the processors (Section V-C). Finally, 2-D ambiguity functions for the processors are presented and analyzed (Section V-D).

B. Environmental Sensitivity and Sampling

A set of tests were run to compare the sensitivity to environmental change of the MVDR, Bartlett, and adaptive minmax matched field processors. In addition, the effect of the density of the sampling of the range of environmental conditions (Φ) on the performance of the adaptive minmax matched field processor was evaluated. For these tests, a single source was located at a depth of 150 m and a range of 100 km, and the actual surface sound speed was varied between 1488 and 1483 m/s.

A total of six processors were tested. The processors were environmentally matched MVDR and Bartlett matched field processors, environmentally mismatched MVDR and Bartlett matched field processors, and three-point and five-point adaptive minmax matched field processors. In each test, the environmentally matched MVDR and Bartlett processors were provided with the true value of the surface sound speed, while the mismatched MVDR and Bartlett processors were given a value of 1487 m/s for the surface sound speed. The three-point processor used three samples of the set Φ at 1487, 1485, and 1483 m/s, while the five-point processor used samples at 1487, 1486, 1485, 1484, and 1483 m/s.

The array focal point was swept in range and depth around the actual source location, and the location and value of the peak response were noted. If the location of the peak response was significantly different from the true source location, the processor response at the true source location was also recorded. The loss in peak response of the mismatched MVDR and Bartlett and adaptive minmax processors, when compared to the peak response of the matched processors, is a measure of the signal loss due to environmental mismatch or uncertainty. The displacement of the peak response position away from the true source position is a measure of the bias in source location estimation due to environmental mismatch.

Table I lists the peak response loss of the mismatched MVDR and Bartlett processors and the two minmax processors as a function of the actual surface sound speed (c_{surf}). For the cases of the MVDR and the minmax processors, the peak

TABLE I
PEAK RESPONSE LOSS FOR VARIOUS PROCESSORS VERSUS c_{surf}

c_{surf} (m/s)	mismatched MVDR (dB)	mismatched Bartlett (dB)	3-pt Minmax (dB)	5-pt Minmax (dB)
1488.00	-5.23	-0.15	-5.23	-5.23
1487.75	-3.62	-0.08	-3.62	-3.62
1487.50	-1.96	-0.03	-1.96	-1.96
1487.25	-0.56	-0.01	-0.56	-0.56
1487.00	0.00	0.00	-0.02	-0.02
1486.75	-0.61	-0.01	-0.15	-0.07
1486.50	-1.97	-0.03	-0.33	-0.08
1486.25	-3.57	-0.07	-0.43	-0.06
1486.00	-5.10	-0.14	-0.50	-0.04
1485.50	-7.61	-0.32	-0.32	-0.10
1485.00	-9.65	-0.57	-0.06	-0.06
1484.00	$\frac{-7.24}{-13.03}$	$\frac{-0.52}{-1.67}$	-0.57	-0.07
1483.00	$\frac{-6.28}{-15.27}$	$\frac{-0.21}{-3.90}$	-0.02	-0.02

loss is with respect to the matched MVDR processor; and for the mismatched Bartlett processor, the peak loss is with respect to the matched Bartlett processor. (The peak response of the matched Bartlett processor was 0.07 dB above that of the matched MVDR processor. This reflects the superior ability of the MVDR processor to reject the surface-generated noise.) In all cases except for the mismatched MVDR and Bartlett processors when the actual surface sound speed is 1484 or 1483 m/s, the peak displacement is less than 1.4 m. For those two cases, the peak displacement is approximately 74 m. The two values listed in Table I for these cases are the peak response and the response at the true source location, respectively.

These results clearly show the serious performance degradation of the MVDR processor and the moderate performance degradation of the Bartlett processor as the actual surface sound speed varies from that assumed by the processor.

The results generated with the minmax processors highlight several important points. First, when the actual surface sound speed falls outside the specified environmental operating range (Φ), the processor's performance experiences the same degradation as the MVDR processor. This is to be expected because when the actual environmental condition is outside Φ, the processor is unable to find a replica vector within the convex hull of the replica vectors corresponding to the sample points of Φ which matches the actual replica vector. Referring to the two-stage MVDR processor interpretation of the minmax processor, this results in a mismatch between the actual and effective replica vectors in the second-stage MVDR processor. Therefore, in this case, the Minmax and standard MVDR processors exhibit the same performance degradation.

The results also clearly show that when the surface sound speed variations fall within the environmental operating range (Φ), the minmax processor has a minimal performance loss. Note that when c_{surf} equals 1486 m/s, the difference between the actual surface sound speed and nearest sample points of the set Φ for the three-point minmax processor (1487 and 1485 m) is 1 m/s. The peak response loss for the three-point processor in this case is -0.50 dB. Under these same conditions, the mismatched processors also have a surface sound speed mismatch of 1 m/s and the mismatched MVDR processor has a peak response loss of -5.10 dB. This improved robustness of the minmax processor is due to the fact that the processor can use any vector within the convex hull of the set of replica vectors corresponding to the sample points of Φ (i.e., $\tilde{Q}(f,r,z)$) as the effective replica vector. Thus, an effective replica vector, which is close to the actual replica vector, can be constructed using a convex combination of the replica vectors corresponding to surface sound speeds of 1487, 1485, and 1483 m/s. The minmax processor's use of all of the vectors in the convex hull of $\tilde{Q}(f,r,z)$ makes it possible to achieve a reasonable level of robustness with a limited number of sample points of Φ.

While the peak response loss of the Bartlett processor is comparable to that of the minmax processor for small surface sound speed mismatches (< 1 m/s), the results in the following two subsections show that resolution and the sidelobe control of the Bartlett processor are far inferior to those of the minmax processor.

C. Spatial Resolution

The next results allow for a quantitative comparison of the spatial resolutionof the matched MVDR, matched Bartlett, and the five-point adaptive minmax processors. In order to compare the vertical spatial resolution, two equal-strength sources were placed at a range of 100 km and a depth of $150 \pm \Delta_{\text{depth}}$ m where $2\Delta_{\text{depth}}$ is the depth separation between the two sources. In order to compare the horizontal spatial resolution, two equal-strength sources were placed at a depth of 150 m and a range of $100\,000 \pm \Delta_{\text{range}}$ m where $2\Delta_{\text{range}}$ is the range separation between the sources. Fig. 5 shows characteristic ambiguity functions as a function of depth evaluated at a range of 100 km. In the case of Fig. 5(a), the processor is able to resolve the two sources, while in the case of Fig. 5(b), the processor is unable to resolve the two sources.

As a quantitative measure of the processor's ability to resolve two sources, the response ratio, which is defined as $10 \log_{10}(\hat{\sigma}_m^2) - 10 \log_{10}(\hat{\sigma}_s^2)$, is used. The definitions of $\hat{\sigma}_m^2$ and $\hat{\sigma}_s^2$ depend on whether or not the processor is able to

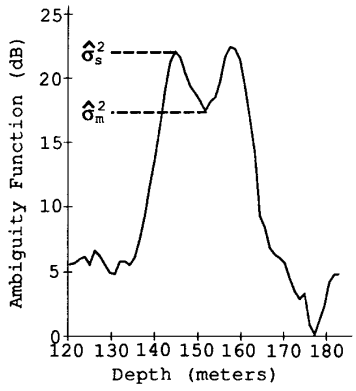

(a)

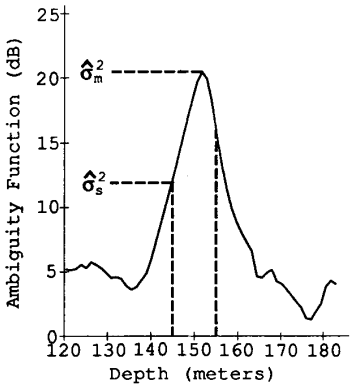

(b)

Fig. 5. Ambiguity functions for two source separations: (a) Two sources resolved; (b) two sources not resolved.

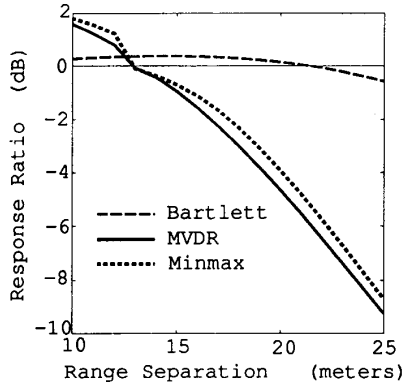

(a)

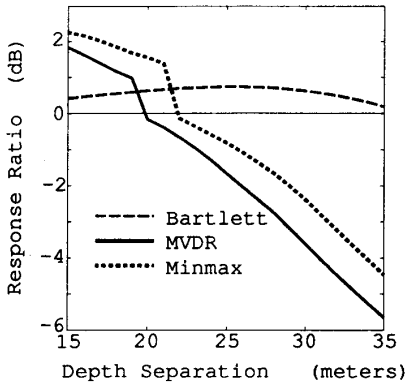

(b)

Fig. 6. Response ratio versus source separations: (a) Horizontal resolution; (b) vertical resolution.

resolve the two sources. In the case of Fig. 5(a) where the processor is able to resolve the two sources, $\hat{\sigma}_m^2$ is defined as the minimal value of the ambiguity function between the two peaks and $\hat{\sigma}_s^2$ is defined as the smaller of the two peak values. In the case of Fig. 5(b) where the processor is not able to resolve the two sources, $\hat{\sigma}_m^2$ is defined as the peak value of the ambiguity function between the two source locations and $\hat{\sigma}_s^2$ is defined as the smaller of the values of the ambiguity function evaluated at the two source locations. The vertical lines in Fig. 5(b) mark the two source depths of 145 and 155 m. If the response ratio is positive, the processor is not able to resolve the two sources; and if it is negative, the processor is able to resolve the two sources. The more negative the value of the response ratio, the deeper the valley in the ambiguity function between the two peaks and the easier it is for the processor to resolve the sources.

Fig. 6(a) and 6(b) show the response ratios for the MVDR, Bartlett, and minmax processors as a function of range and depth separation, respectively. The spatial resolution of the adaptive minmax processor can be seen to be substantially superior to that of the matched Bartlett processor and marginally inferior to that of the matched MVDR processor. The loss of resolution with respect to the matched MVDR processor can be attributed to the lack of precise environmental information available to the Minmax processor.

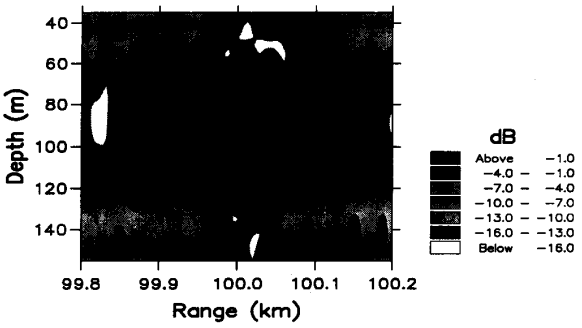

Fig. 7. Ambiguity function for matched Bartlett processor.

D. Ambiguity Functions

Finally, the 2-D ambiguity functions for each of the processors are presented for visual analysis. A source was simulated at a range of 100 km and a depth of 95 m. The actual surface sound speed was 1484.75 m/s and the mismatched processors were given a value of 1487 m/s for the surface sound speed. The adaptive minmax processor utilized five samples of the set Φ as described in Section V-B. Figs. 7–11 show the ambiguity functions covering the ranges of 99.8–100.2 km and the depths of 35–155 m.

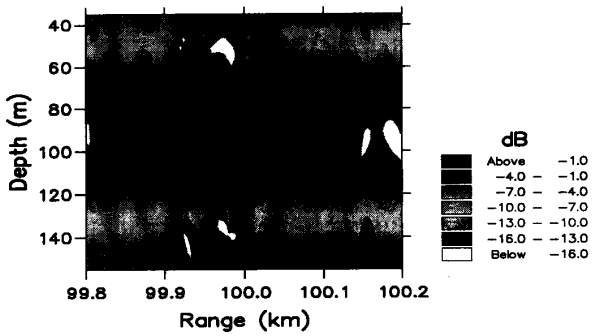

Fig. 8. Ambiguity function for mismatched Bartlett processor.

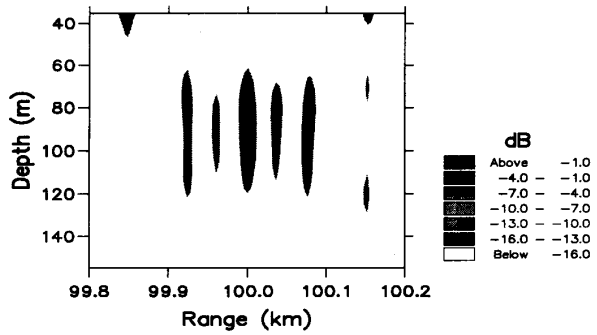

Fig. 9. Ambiguity function for matched MVDR processor.

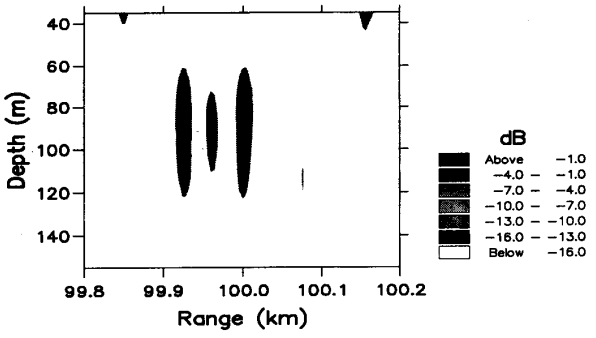

Fig. 10. Ambiguity function for mismatched MVDR processor.

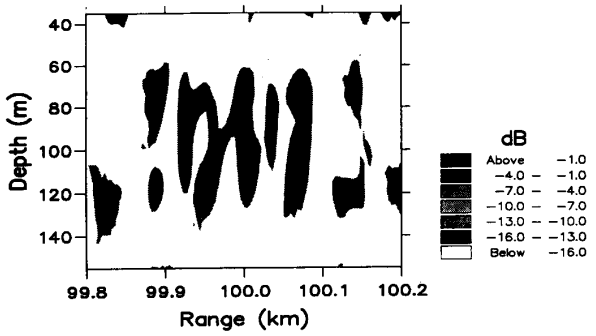

Fig. 11. Ambiguity function for adaptive minmax processor.

The figures clearly show the superior spatial resolution of the MVDR and adaptive minmax processors with respect to the Bartlett processor, and the reduced requirement by the adaptive minmax processor for precise environmental information when compared to the MVDR processor. The peak response levels for the matched Bartlett, mismatched Bartlett, matched MVDR, mismatch MVDR, and adaptive minmax processors are $0, -.30, -0.5, -6.76$, and -0.09 dB, respectively. The peak response locations for the matched Bartlett, matched MVDR, and adaptive minmax processors are at the actual source location. The peak response locations for the mismatched Bartlett and MVDR processors are at the actual source depth, but are displaced by approximately 76 m in range from the actual source location. This peak displacement for the mismatched processors correlates closely with the peak displacement found for some of the cases considered in Section V-B. The displaced peak location corresponds to a location where the replica vector for the assumed environmental conditions closely matches the replica vector for the actual source location and environmental condition.

It is interesting to note that the adaptive minmax processor has a sidelobe peak of -6.76 dB at the same location as the displaced peaks of the ambiguity functions of the mismatched processors (95 m depth, 99.925 km range). This sidelobe highlights a fundamental ambiguity which can affect the performance of a processor which has only approximate environmental information. In this case, the replica vector corresponding to a surface sound speed of 1487 m/s and a source location of 95 m depth and 99.925 km range closely matches that corresponding to a surface sound speed of 1484.75 m/s and a source location of 95 m depth and 100 km range. Both environmental conditions fall within the range of environmental conditions over which the adaptive minmax processor is designed to operate. Therefore, when focusing at the sidelobe location, the processor finds that one surface sound speed within the designated range yields a signal replica vector which closely matches the observed spatial structure of the received signal. This results in a sidelobe peak in the processors response at this location. Such a fundamental ambiguity will exist whenever multiple environment/source location pairs yield approximately equal signal replica vectors, and it accounts for the generally higher sidelobe levels in the ambiguity function of the adaptive minmax processor when compared to those of the MVDR processor.

VI. Conclusions

Many array processors experience environmental mismatch because they do not have access to accurate and precise environmental information. This environmental mismatch results in a signal model mismatch which itself leads to a severe degradation in performance in many adaptive processors. The adaptive minmax matched field processor has been proposed. Its spatial resolution is close to that achieved by adaptive processors operating with complete environmental information, while at the same time requiring only approximate environmental information and exhibiting none of the sensitivity to environmental mismatch which is characteristic of the adaptive processors.

The central element of the processor is a linear weight-and-sum beamformer, the weights of which are the solution to a particular minmax problem. Two theorems have been derived which allow the problem of finding the optimal minmax array weights to be recast as a linearly constrained quadratic programming problem for which an efficient, finite convergence algorithm is available. In addition, the theorems also motivate the interpretation of the minmax processor as a joint signal replica vector estimator/MVDR matched field processor. This interpretation relates the minmax processor to the traditional MVDR processor, motivates a modification to the minmax processor, and aids in the analysis of the minmax processor.

ACKNOWLEDGMENT

The author thanks Prof. A. V. Oppenheim and Prof. A. B. Baggeroer from M.I.T. for the significant contributions, both technical and nontechnical, which they made to the completion of this work. Their collective insights, knowledge, skepticism, and concern have been greatly appreciated and valued.

REFERENCES

[1] H. Cox, "Resolving power and sensitivity to mismatch of optimum array processors," *J. Acoust. Soc. Amer.*, vol. 54, pp. 771–785, Mar. 1973.
[2] D. F. Gingras, "Methods for predicting the sensitivity of matched-field processors to mismatch," *J. Acoust. Soc. Amer.*, vol. 86, pp. 1940–1949, Nov. 1989.
[3] E.-C. Shang and Y. Y. Wang, "Environmental mismatching effects on source localization processing in mode space," *J. Acoust. Soc. Amer.*, vol. 89, pp. 2285–2290, May 1991.
[4] A. B. Baggeroer, W. A. Kuperman, and H. Schmidt, "Matched field processing; Source localization in correlated noise as an optimum parameter estimation problem," *J. Acoust. Soc. Amer.*, vol. 83, pp. 571–587, Feb. 1988.
[5] J. Capon, "High resolution frequency-wavenumber spectrum analysis," *Proc. IEEE*, vol. 57, pp. 1408–1418, Aug. 1969.
[6] P. J. Huber, "Robust estimation of a location parameter," *Ann. Math. Statist.*, vol. 35, pp. 73–101, 1964.
[7] S. A. Kassam and T. L. Lim, "Robust Wiener filters," *J. Franklin Inst.*, vol. 304, pp. 171–185, Oct./Nov. 1977.
[8] H. V. Poor, "Uncertainty tolerance in underwater acoustic signal processing," *IEEE J. Oceanic Eng.*, vol. OE-12, pp. 48–65, Jan. 1987.
[9] K. S. Vastola and H. V. Poor, "Robust Wiener–Kolmogorov theory," *IEEE Trans. Inform. Theory*, vol. IT-30, pp. 316–327, Mar. 1984.
[10] S. Verdu and H. V. Poor, "On minmax robustness: A general approach and applications," *IEEE Trans. Inform. Theory*, vol. IT-30, pp. 328–340, Mar. 1984.
[11] D. F. Gingras and N. L. Geer, "Minimax robust matched-field processing," *J. Acoust. Soc. Amer.*, vol. 93, pp. 2798–2808, May 1993.
[12] J. C. Preisig, "Adptive matched field processing in an uncertain propagation environment," RLE Tech. Rep. 567, M.I.T., Cambridge, Jan. 1992.
[13] L. B. Dozier and F. D. Tappert, "Statistics of normal mode amplitudes in a random ocean. I. Theory," *J. Acoust. Soc. Amer.*, vol. 63, pp. 353–365, Feb. 1978.
[14] ——, "Statistics of normal mode amplitudes in a random ocean. II. Computations," *J. Acoust. Soc. Amer.*, vol. 64, pp. 533–547, Aug. 1978.
[15] S. M. Flatte, *Sound Transmission Through a Fluctuating Ocean*. Cambridge, England: Cambridge Univ. Press, 1979.
[16] C. E. Lemke, "On complementary pivot theory," in X. Dantzig and X. Veinott, Ed., *Mathematics of the Decision Sciences, Part 1*. Providence, RI: Amer. Math. Soc., 1968, pp. 95–114.
[17] M. S. Bazaraa and C. M. Shetty, *Nonlinear Programming, Theory and Applications*. New York: Wiley, 1979.
[18] B. Eaves, "The linear complementarity problem," *Management Sci.*, vol. 11, pp. 612–634, May 1971.
[19] K. G. Murty, *Linear Complementarity, Linear and Nonlinear Programming*. Heldermann Verlag, 1988.
[20] M. Abramowitz and I. A. Stegun, *Handbook of Mathematical Functions*. Washington, DC: Nat. Bureau of Standards Appl. Math. Ser. 55, U.S. Dep. Commerce, 1972.
[21] G. V. Frisk, *Ocean and Seabed Acoustics*. Englewood Cliffs, NJ: Prentice-Hall, 1993.
[22] I. Tolstoy and C. S. Clay, *Ocean Acoustics, Theory and Experiment in Underwater Sound*. New York: McGraw-Hill, 1966.
[23] W. A. Kuperman and F. Ingenito, "Spatial correlation of surface generated noise in a stratified ocean," *J. Acoust. Soc. Amer.*, vol. 67, pp. 1988–1996, June 1980.

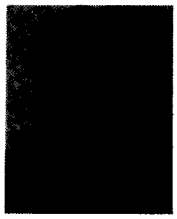

James C. Preisig received the B.S. degree in electrical engineering from the United States Coast Guard Academy in 1980, the S.M. and E.E. degrees in electrical engineering from the Massachusetts Institute of Technology in 1988, and the Ph.D. degree in electrical and ocean engineering from the Massachusetts Institute of Technology/Woods Hole Oceanographic Institution Joint Program in Oceanography/Oceanographic Engineering in 1992.

Since 1992 he has been a Postdoctoral Investigator at the Woods Hole Oceanographic Institution. He is currently also an Adjunct Professor at Northeastern University and a Research Affiliate at the Massachusetts Institute of Technology. From 1980 to 1985 he served on active duty in the United States Coast Guard. From 1986 to 1989 he held a National Science foundation Graduate Fellowship, and from 1989 to 1990 he held a General Electric Foundation Graduate Fellowship in Electrical Engineering. His research interests include the development of signal design, modeling, and processing techniques to address problems related to acoustics and oceanography.